Interactions of Metal Ions with Water: Ab Initio Molecular Orbital Studies of Structure, Bonding Enthalpies, Vibrational Frequencies and Charge Distributions. 1. Monohydrates

Mendel Trachtman,[†] George D. Markham,[‡] Jenny P. Glusker,[‡] Philip George,[‡] and Charles W. Bock*,[†,‡]

Department of Chemistry, Philadelphia College of Textiles and Science, Henry Avenue and School House Lane, Philadelphia, Pennsylvania 19144, and The Institute for Cancer Research, Fox Chase Cancer Center, 7701 Burholme Avenue, Philadelphia, Pennsylvania 19111

Received December 29, 1997

The formation and properties of a wide range of metal ion monohydrates, $M^{n+}-OH_2$, where $n = 1$ and 2, have been studied by ab initio molecular orbital calculations at the MP2(FULL)/6-311++G**//MP2(FULL)/6-311++G** and CCSD(T)(FULL)/6-311++G**//MP2(FULL)/6-311++G** computational levels. The ions M are from groups 1A, 2A, 3A, and 4A in the second, third, and fourth periods of the periodic table and the first transition series. Structural parameters, vibrational frequencies, bonding enthalpies, orbital occupancies and energies, and atomic charge distributions are reported. Trends in these properties are correlated with the progressive occupancy of the *s*, *p*, and *d* orbitals. Except for K^+-OH_2 and $Ca^{2+}-OH_2$, the O−H bond lengths and HOH angles are greater in the hydrates than in unbound water. The M−O bond lengths decrease proceeding from group 1A → 4A but become larger in proceeding from the second → fourth period. The bonding enthalpies, ΔH°_{298}, are found to be inversely linearly dependent on the M−O bond length M^{n+} according to equations of the form $\Delta H^\circ_{298} = A + B(1/M-O)$ for $n = 1$ and $n = 2$. Within each monohydrate the distribution of atomic charge reveals a small but definite transfer of charge from water to the metal ion. Compared to unbound water there is, in a metal-ion-bound water complex, an *increase* in the electronic (negative) charge on the oxygen atom, accompanied by a (significantly) *larger decrease* in the electronic charge on the hydrogen atoms. The bonding of the water molecule, although electrostatic in origin, is thus more complex than a simple interaction between a point charge on the metal ion, and the water dipole.

Introduction

The interaction of metal cations with neutral ligands, such as water, occurs in a wide variety of physical, chemical, and biological phenomena.[1] For example, one-third of all proteins require a metal ion for their structure and/or function:[2] and many of these protein-bound metal ions are bonded to at least one water molecule.[3] Furthermore, metalloenzymes are often active only when the metal ion is a specific one. In several enzyme systems the catalytic activity involves deprotonation of a metal ion-bonded water molecule giving a hydroxyl group, which then acts as a nucleophile that can attack the substrate.[4] Knowledge of the fundamental nature of the metal ion−water bonding and the deprotonation process is therefore necessary for a full understanding of the mechanism of action of such enzymes.

Deprotonation has long been known as a characteristic property of water when bound to a metal ion. Metal ion hydrates are only stable in a moderately acidic solution. At higher pH values an "ion-pair" complex, such as the monohydroxide, $M^{n+}[OH]^-$ is formed, and at still higher pH values the polyhydroxide $M^{n+}[OH]^-_n$ is precipitated.[5,6]

The importance of the metal ion−water interaction has led to extensive computational molecular orbital studies by many investigators of hydrates of metal ions ranging over much of the periodic table.[7−12] Many have concentrated on the physical and/or chemical properties of metal ion hydrates with multiple water molecules, e.g., clusters such as $Be[H_2O]^{2+}_4$, $Ca[H_2O]^{2+}_6$, $Mn[H_2O]^{2+}_6$, and $Zn[H_2O]^{2+}_6$.[13−17] Other studies have explored the properties of the monohydrates in a specific

* To whom correspondence should be addressed.
[†] Philadelphia College of Textiles and Science.
[‡] Fox Chase Cancer Center.

(1) Silva, J. J. R. Fd.; Williams, R. J. P. *The Biological Chemistry of the Elements*; Clarendon Press: Oxford, 1991.
(2) Trainer, J. A.; Roberts, V. A.; Getzoff, E. D. *Curr. Opin. Biotechnol.* **1991**, *2*, 582−590.
(3) Katz, A. K.; Glusker, J. P.; Beebe, S. A.; Bock, C. W. *J. Am. Chem. Soc.* **1996**, *118*, 5752−5763.
(4) Whitlow, M.; Howard, A. J. *Trans. Am. Crystallogr. Assoc.* **1991**, 25−126.
(5) Nancollas, G. H. *Q. Rev. Chem. Soc.* (*London*) **1960**, *14*, 402−426.
(6) *Stability Constants of Metal-Ion Complexes. Section I. Inorganic Ligands*; compiled by Sillen, L. G.; Special Publication 17; Chemical Society: London, 1964; pp 39−84 and references therein.
(7) Hermansson, K.; Olovsson, I. *Theor. Chim. Acta* (*Berlin*) **1984**, *64*, 265−276.
(8) Rosi, M.; Bauschlicher, C. W., Jr. *J. Chem. Phys.* **1989**, *90*, 7264−7272.
(9) Rosi, M.; Bauschlicher, C. W., Jr. *J. Chem. Phys.* **1990**, *92*, 1876−1878.
(10) Bauschlicher, C. W., Jr.; Langhoff, S. R.; Partridge, H. In *Modern Electronic Structure Theory, Part I*; Yarkony, D. R., Ed.; World Scientific: Singapore, 1997; pp 1312−1318.
(11) Glendening, E. D.; Feller, D. *J. Phys. Chem.* **1995**, *99*, 3060−3067.
(12) Feller, D.; Glendening, E. D.; Kenddall, R. A.; Peterson, K. A. *J. Chem. Phys.* **1994**, *100*, 4981−4997.
(13) Hashimoto, K.; Yoda, N.; Iwata, S. *Chem. Phys.* **1987**, *116*, 193−202.
(14) Bock, C. W.; Glusker, J. P. *Inorg. Chem.* **1993**, *32*, 1242−1250.
(15) Bock, C. W.; Kaufman, A.; Glusker, J. P. *Inorg. Chem.* **1994**, *33*, 419−427.
(16) Bock, C. W.; Katz, A. K.; Glusker, J. P. *J. Am. Chem. Soc.* **1995**, *117*, 3754−3765.

S0020-1669(97)01613-3 CCC: $15.00
Published on Web 07/24/1998

Table 1. Electronic Configurations of the Ground State and Low-Lying Excited States of the Transition Metal Ion Monohydrates, $M^{+}-OH_2$ and $M^{2+}-OH_2$, Together with the Energies (kcal/mol) Relative to the Ground State, Calculated Using the MP2(FULL)/6-311++G**// MP2(FULL)/6-311++G** and {CCSD(T)(FULL)/6-311++G**//MP2(FULL)/6-311++G**} Computational Levels; the Coordinate System is Shown in Figure 1

hydrate	state	orbital occupancy	relative energy (kcal/mol)
$Sc^{+}-OH_2$	$^3A_1$	(4s, $d_{x^2-y^2}$)	zero {zero}
	$^3A_2$	(4s, d_{xy})	+0.01 {+0.08}
	$^3B_2$	(4s, d_{yz})	+3.39
	$^3B_1$	(4s, d_{xz})	+6.46 {+0.08}
$Sc^{2+}-OH_2$	$^2A_1$	($d_{x^2-y^2}$)	zero {zero}
	$^2A_2$	(d_{xy})	+0.06 {+0.19}
$Ti^{+}-OH_2$	$^4B_2$	(4s, d_{yz}, $d_{x^2-y^2}$)	zero {zero}
	$^4B_1$	(4s, d_{xy}, d_{yz})	+1.05 {+0.79}
	$^4B_1$	(4s, $d_{x^2-y^2}$, d_{xz})	+3.68 {+3.84}
	$^4A_2$	(4s, d_{xz}, d_{yz})	+9.09 {+8.31}
$Ti^{2+}-OH_2$	$^3B_2$	(d_{yz}, $d_{x^2-y^2}$)	zero {zero}
	$^3B_1$	(d_{xy}, d_{yz})	+2.15 {+1.31}
	$^3A_2$	(d_{xy}, $d_{x^2-y^2}$)	+15.02
$V^{+}-OH_2$	$^5A_1$	(4s, d_{xy}, d_{xz}, d_{yz})	zero {zero}
	$^5A_2$	(4s, d_{xz}, d_{yz}, $d_{x^2-y^2}$)	+0.07 {+0.21}
$V^{2+}-OH_2$	$^4A_2$	(d_{xz}, d_{yz}, $d_{x^2-y^2}$)	zero {zero}
	$^4A_1$	(d_{xy}, d_{xz}, d_{yz})	+0.02 {+0.03}
$Cr^{2+}-OH_2$	$^5A_1$	(d_{xy}, d_{yz}, d_{xz}, $d_{x^2-y^2}$)	zero
	$^5B_1$	(d_{xy}, d_{yz}, $d_{x^2-y^2}$, d_{z^2})	+8.59
	$^5A_2$	(d_{xz}, d_{yz}, $d_{x^2-y^2}$, d_{z^2})	+15.83
$Mn^{+}-OH_2$	$^7A_1$	(4s, d_{xy}, d_{xz}, d_{yz}, $d_{x^2-y^2}$, d_{z^2})	zero {zero}
	$^5A_1$	(4s, d_{xy}, d_{xz}, d_{yz}, $d_{x^2-y^2}$, d_{z^2})[a]	+25.22 {+15.72}
$Fe^{+}-OH_2$	$^4B_2$	(d_{xy}, d_{xz}, d^2_{yz}, $d^2_{x^2-y^2}$, d_{z^2})	zero {+3.68}
	$^4B_1$	(d^2_{xy}, d_{xz}, d^2_{yz}, $d_{x^2-y^2}$, d_{z^2})	+5.21 {+6.04}
	$^6A_1$	(4s, d_{xy}, d_{xz}, d_{yz}, $d^2_{x^2-y^2}$, d_{z^2})	+9.60 {zero}
	$^4A_1$	(4s, d_{xy}, d_{xz}, d_{yz}, $d^2_{x^2-y^2}$, d_{z^2})[b]	+26.09 {+2.07}
$Fe^{2+}-OH_2$	$^5A_1$	(d_{xy}, d_{xz}, d_{yz}, $d^2_{x^2-y^2}$, d_{z^2})	zero {zero}
	$^5A_2$	(d^2_{xy}, d_{xz}, d_{yz}, $d_{x^2-y^2}$, d_{z^2})	+0.05 {+0.70}
	$^5B_2$	(d_{xy}, d_{xz}, d^2_{yz}, $d_{x^2-y^2}$, d_{z^2})	+3.01
$Co^{+}-OH_2$	$^3B_1$	(d^2_{xy}, d_{xz}, d^2_{yz}, $d_{x^2-y^2}$, $d^2_{z^2}$)	zero {+0.33}
	$^3A_2$	(d_{xy}, d^2_{xz}, d^2_{yz}, $d^2_{x^2-y^2}$, d_{z^2})	+0.42 {zero}
	$^3A_1$	(d^2_{xy}, d^2_{xz}, d^2_{yz}, $d_{x^2-y^2}$, d_{z^2})	0.47 {+0.04}
	$^3A''$	(d^2_{xy}, d^2_{xz}, d_{yz}, $d_{x^2-y^2}$, $d^2_{z^2}$)[c]	+2.09
	$^3A_2$	(d^2_{xy}, d_{xz}, d_{yz}, $d^2_{x^2-y^2}$, $d^2_{z^2}$)	+8.25 {+6.18}
$Co^{2+}-OH_2$	$^4B_2$	(d_{xy}, d_{xz}, d^2_{yz}, $d^2_{x^2-y^2}$, d_{z^2})	zero {zero}
	$^4B_1$	(d_{xy}, d^2_{xz}, d_{yz}, $d^2_{x^2-y^2}$, d_{z^2})	+3.66 {+4.45}
	$^4B_1$	(d^2_{xy}, d_{xz}, d^2_{yz}, $d_{x^2-y^2}$, d_{z^2})	+4.62
	$^4A_2$	(d^2_{xy}, d_{xz}, d_{yz}, $d_{x^2-y^2}$, $d^2_{z^2}$)	+7.77
	$^4A_2$	(d_{xy}, d^2_{xz}, d^2_{yz}, $d_{x^2-y^2}$, d_{z^2})	+12.50
$Ni^{+}-OH_2$	$^2A_1$	(d^2_{xy}, d^2_{xz}, d^2_{yz}, $d^2_{x^2-y^2}$, d_{z^2})	zero {zero}
	$^2B_1$	(d^2_{xy}, d_{xz}, d^2_{yz}, $d^2_{x^2-y^2}$, $d^2_{z^2}$)	+2.24 {+2.36}
	$^2A_2$	(d_{xy}, d^2_{xz}, d^2_{yz}, $d^2_{x^2-y^2}$, $d^2_{z^2}$)	+4.08
$Ni^{2+}-OH_2$	$^3A_1$	(d^2_{xy}, d^2_{xz}, d^2_{yz}, $d_{x^2-y^2}$, d_{z^2})	zero {zero}
	$^3A_2$	(d^2_{xy}, d_{xz}, d_{yz}, $d^2_{x^2-y^2}$, $d^2_{z^2}$)	+2.73 {+1.71}
$Cu^{2+}-OH_2$	$^2A_1$	(d^2_{xy}, d^2_{xz}, d^2_{yz}, $d^2_{x^2-y^2}$, d_{z^2})	zero {zero}
	$^2B_1$	(d^2_{xy}, d_{xz}, d^2_{yz}, $d^2_{x^2-y^2}$, $d^2_{z^2}$)	+7.93 {+8.51}
	$^2A_1$	(d_{xy}, d^2_{xz}, d^2_{yz}, $d^2_{x^2-y^2}$, $d^2_{z^2}$)	+15.26 {+18.74}

[a] All 3d orbitals α-spin: 4s orbital β-spin. [b] 4s orbital β-spin. [c] Bent.

group, e.g., the alkali metals,[11,12] or in a particular row, e.g., the monovalent first row transition metals.[8,9] Still other studies have examined the energetic consequences of sequential hydration, where the results can be compared directly with experiment.[18]

To gain more insight into the factors involved in the deprotonation we have carried out ab initio molecular orbital calculations at the MP2(FULL)/6-311++G**//MP2(FULL)/6-311++G** and CCSD(T)(FULL)/6-311++G**//MP2(FULL)/6-311++G** levels on the metal ions, M^{n+}, the monohydrates,

(17) Katz, A. K.; Glusker, J. P.; Beebe, S. A.; Bock, C. W. *J. Am. Chem. Soc.* **1996**, *118*, 5752−5763.

(18) Tachikawa, H.; Ichikawa, T.; Yoshida, H. *J. Am. Chem. Soc.* **1990**, *112*, 982−987.

$M[H_2O]^{n+}$, and the monohydroxides, $M[OH]^{(n-1)+}$. In the present paper, we report structural parameters, bonding enthalpies, vibrational frequencies, orbital occupancy and atomic charges for a wide variety of monohydrates, where the metal ions, M^{n+}, are taken from the second, third and fourth rows of the periodic table, and the formal charge on the metal, *n*, is 1 or 2. Results for boron, carbon and silicon (although not metal ions) are also included so that trends in these various properties can be related to the progressive occupancy of the s, p, and d shells. These results represent studies done consistently on all metal ions under the same conditions, and therefore are suitable for comparative analyses.

The deprotonation of metal hydrates can be expressed as

$$M[H_2O]^{n+} \rightarrow M[OH]^{(n-1)+} + H^+,$$

or as a proton-transfer reaction

$$M[H_2O]^{n+} + H_2O \rightarrow M[OH]^{(n-1)+} + H_3O^+$$

Deprotonation would be favored by stronger bonding in the hydroxide in relation to the weaker bonding in the hydrate. The interplay between the factors which bring about the bonding of H_2O, and the bonding of OH^- to metal ions, are thus key elements in understanding the natural selection of one or the other particular metal ion for a specific enzyme system. The most likely ions to be involved in biochemical systems are those that are stable in water, namely the divalent cations Be^{2+}, Mg^{2+}, Ca^{2+}, Mn^{2+}, Fe^{2+}, Co^{2+}, Cu^{2+}, Zn^{2+}, and the trivalent cations Al^{3+}, Cr^{3+}, Mn^{3+}, and Fe^{3+}, since, in principle at least, they could be readily accessible from an aqueous environment for bonding to the protein. It is well-established that Mg^{2+}, Ca^{2+}, and Zn^{2+} play such a role.[16,17,19] The present study is the first stage in the investigations of such a process.

Prior to 1989, experimental values of the binding enthalpies for $M[H_2O]^+$ were available only for the alkali metal ions Li^+, Na^+, K^+, Rb^+, and Cs^+;[20] dissociation energies of the transition metal ion complexes $Cu[H_2O]_n^+$) ($n = 3-5$) had also been reported.[21−23] In 1989, however, three papers appeared, all based on collision-induced dissociation (CID) experiments, that expanded the available binding enthalpies to include all the *monovalent* first-row transition metals.[24−26] In 1994, Dalleska et al.[27] reported revised values of the hydration enthalpies for these transition metals, based on CID experiments in a guided ion beam mass spectrometer, and the error bars on these values were significantly smaller than those from earlier results.[24−26] As first noted by Corongiu and Clementi,[28] *divalent* cations can behave differently than singly charged ions, when interacting with water. Specifically, the dissociation products of $M[H_2O]^{2+}$ may be $M^+ + H_2O^+$ instead of $M^{2+} + H_2O$, owing to the relative magnitudes of the ionization potentials for the metal ion and water. Curtiss et al.[29] calculated that for $Fe[H_2O]^{2+}$ the crossover between the two dissociation pathways occurs only for an Fe−O distance greater than 6 Å. Unfortunately, very little direct experimental data is currently available concerning either pathway for most divalent metal ions.

Computational Methods

Ab initio molecular orbital calculations were performed at the MP2(FULL)/6-311++G**//MP2(FULL)/6-311++G** level[30,31a−e] on the CRAY YMP computer at the National Cancer Institute and DEC alpha 3000/600 and SGI origin 2000 workstations using the GAUSSIAN 94 program[32] on the metal ions, M^{n+}, and the monohydrates, $M[H_2O]^{n+}$, with $n = 1$ and 2. Since 6-311++G** basis sets for potassium and calcium are not available in GAUSSIAN 94, calculations on $K[H_2O]^+$ and $Ca[H_2O]^{n+}$ ($n = 1,2$) were carried out using Huzinaga <4,3,3,2,1/4,3> basis sets,[33] augmented by two *p*-type and two *d*-type polarization functions and one *sp*-type diffuse function on the potassium and calcium atoms. The 6-311++G** basis set was still used for the oxygen and hydrogen atoms: six d-type functions were used only in these two cases. As noted by Kaupp and Schleyer,[34] d orbitals and core polarization are both important for cationic d^0 metal complexes such as $Ca[H_2O]^{2+}$. Spin projected energies were used where appropriate, and spin conservation was assumed in all complex formation reactions. Complete optimizations were performed on all the monohydrates, and frequency analyses were carried out to confirm that the reported structures are local minima on the MP2(FULL)/6-311++G** potential energy surface, and to evaluate the thermal energy contributions necessary for the calculations of enthalpy changes for the hydration reaction

$$M^{n+} + H_2O \rightarrow M[H_2O]^{n+}$$

at 298 K. Since calculations at the MP2(FULL)/6-311++G** level do not always predict the correct electronic configuration for the ground state of some first-row transition metals,[35] single point CCSD(T)(FULL)/6-311++G**//MP2(FULL)/6-311++G** calculations were performed in selected cases to more accurately treat the effects of electron correlation in the calculation of the bonding enthalpies. Atomic charges were calculated from

(19) Tainer, J. A.; Roberts, V. A.; Getzoff, E. D. *Curr. Opin. Biotechnol.* **1991**, *2*, 582−590.
(20) Dzidic, I.; Kebarle, P. *J. Phys. Chem.* **1970**, *74*, 1466−1474.
(21) Holland, P. M.; Castleman, A. W., Jr. *J. Am. Chem. Soc.* **1980**, *102*, 6174−6175.
(22) Holland, P. M.; Castleman, A. W., Jr. *J. Chem. Phys.* **1982**, *76*, 4195−4205.
(23) Burnier, R. C.; Carlin, T. J.; Reents, W. D., Jr.; Cody, R. B.; Lengel, R. K.; Freiser, B. S. *J. Am. Chem. Soc.* **1979**, *101*, 7127−7129.
(24) Magnera, T. F.; David, D. E.; Stulik, D.; Orth, R. G.; Jonkman, H. T.; Michl, J. *J. Am. Chem. Soc.* **1989**, *111*, 5036−5043.
(25) Magnera, T. F.; David, D. E.; Michl, J. *J. Am. Chem. Soc.* **1989**, *111*, 4100−4101.
(26) Marinelli, P. J.; Squires, R. R. *J. Am. Chem. Soc.* **1989**, *111*, 4101−4103.
(27) Dalleska, N. F.; Honma, K.; Sunderlin, L. S.; Armentrout, P. B. *J. Am. Chem. Soc.* **1994**, *116*, 3519−3528.
(28) Corongiu, G.; Clementi, E. *J. Chem. Phys.* **1978**, *69*, 4885−4887.
(29) Curtiss, L. A.; Halley, J. W.; Hautman, J.; Rahman, A. *J. Chem. Phys.* **1987**, *86*, 2319−2327.
(30) Møller, C.; Plesset, M. S. *Phys. Rev.* **1934**, *46*, 618−622.
(31) (a) McLean, A. D.; Chandler, G. S. *J. Chem. Phys.* **1980**, *72*, 5639−5648. (b) Krishnan, R.; Binkley, J. S.; Seeger, R.; Pople, J. A. *J. Chem. Phys.* **1980**, *72*, 650−654. (c) Wachters, A. J. H. *J. Chem. Phys.* **1970**, *52*, 1033−1036. (d) Hay, P. J. *J. Chem. Phys.* **1977**, *66*, 4377−4384. (e) Raghavachari, K.; Trucks, G. W. *J. Chem. Phys.* **1989**, *91*, 1062−1065.
(32) Frisch, M. J.; Trucks, G. W.; Schlegel, H. B.; Gill, P. M. W.; Johnson, B. G.; Robb, M. A.; Cheeseman, J. R.; Keith, T. A.; Peterson, G. A.; Montgomery, J. A.; Raghavachari, K.; Al-Laham, M. A.; Zakrzewski, V. G.; Ortiz, J. V.; Foresman, J. B.; Cioslowski, J.; Stefanov, B. B.; Nanayakkara, A.; Challacombe, M.; Peng, C. Y.; Ayala, P. Y.; Chen, W.; Wong, M. W.; Andres, J. L.; Replogle, E. S.; Gomperts, R.; Martin, R. L.; Fox, J. S.; Binkley, J. S.; Defrees, D. J.; Baker, J.; Stewart, J. P.; Head-Gordon, M.; Gonzales, C.; Pople, J. A. GAUSSIAN 94, Revision A.1: Gaussian, Inc.: Pittsburgh, PA, 1995.
(33) Huzinaga, S.; Andzelm, J.; Klobukowski, M.; Radzio-Andzelm, E.; Sakai, Y.; Tazewaki, H. *Gaussian Basis Sets for Molecular Calculation*; Elsevier: New York, 1984.
(34) Kaupp, M.; Schleyer, P. v. R. *J. Chem. Phys.* **1992**, *96*, 7316−7323.
(35) Ricca, A.; Bauschlicher, C. W., Jr. *J. Phys. Chem.* **1995**, *99*, 9003−9007.

Table 2. Geometrical Parameters for the Main Group Metal Ion Monohydrates, $M[OH_2]^{n+}$, Calculated at the MP2(FULL)/6-311++G**// MP2(FULL)/6-311++G** and {CCSD(T)(FULL)/6-311++G**//MP2(FULL)/6-311++G**} Computational Levels[a]

			group			
			1A	2A	3A	4A
period	*n*		Li^{n+}	Be^{n+}	B^{n+}	C^{n+}
2	$n = 1$	state	$^1A_1$	$^2A_1$	$^1A_1$	$^2B_2$
		M−O	1.858	1.584	1.524	1.400
		O−H	0.964	0.973	0.982	0.987
		∠HOH	104.9	109.5	113.1	116.5
		ΔH°_{298}	−34.0	−59.8	−49.6	−85.0
			{−33.9}	{−60.6}	{−48.1}	{−82.1}
	$n = 2$	state		$^1A_1$	$^2A_1$	$^1A_1$
		M−O		1.505	1.353	1.288
		O−H		0.992	1.021	1.060
		∠HOH		108.1	112.4	115.8
		ΔH°_{298}		−140.5	−217.9	−239.0
				{−140.4}	{−218.1}	{−235.0}
			Na^{n+}	Mg^{n+}	Al^{n+}	Si^{n+}
3	$n = 1$	state	$^1A_1$	$^2A_1$	$^1A_1$	$^2B_2$
		M−O	2.250	2.091	2.120	1.930
		O−H	0.963	0.967	0.969	0.971
		∠HOH	104.0	105.7	106.2	109.5
		ΔH°_{298}	−23.6	−30.8	−25.9	−43.4
			{−23.5}	{−31.0}	{−26.0}	{−42.4}
	$n = 2$	state		$^1A_1$	$^2A_1$	$^1A_1$
		M−O		1.957	1.842	1.810
		O−H		0.976	0.986	0.994
		∠HOH		105.1	106.9	107.5
		ΔH°_{298}		−77.5	−96.6	−94.5
				{−76.8}	{−96.8}	{−94.6}
			K^{n+}	Ca^{n+}	Ga^{n+}	Ge^{n+}
4	$n = 1$	state	$^1A_1$	$^2A_1$	$^1A_1$	$^2B_2$
		M−O	2.625	2.390	2.288	2.091
		O−H	0.963	0.966	0.966	0.969
		∠HOH	102.9	103.9	105.4	108.6
		ΔH°_{298}	−16.7	−27.6	−23.7	−38.0
			{−17.0}	{−23.9}	{−23.1}	{−36.9}
	$n = 2$	state		$^1A_1$	$^2A_1$	$^1A_1$
		M−O		2.277	1.904	1.973
		O−H		0.972	0.985	0.987
		∠HOH		102.2	108.8	107.4
		ΔH°_{298}		−51.9	−95.1	−81.6
				{−54.6}	{−95.0}	{−80.6}

[a] See Computational Methods for the basis set employed for the K^{n+} and Ca^{n+} calculations. The M−O and O−H bond lengths are in angstroms, the H−O−H bond angles are in degrees, and the bonding enthalpies, ΔH°_{298}, are in kcal/mol. Water [MP2(FULL)/6-311++G**] OH = 0.959 Å, ∠HOH = 103.5°. Water [employed in K^n+ and Ca^n+ calculations, MP2(FULL)/6-311++G**(6D)] OH = 0.960 Å, ∠HOH = 103.4°.

natural population analyses (NPA) using the MP2(FULL)/6-311++G** density. For some of the hydrates, charges were also calculated using the Atoms in Molecules (AIM) method pioneered by Bader[36] and implemented in GAUSSIAN 94 by Ciolowski and co-workers.[37a−c] The effect of basis set superposition error, BSSE, has been discussed by Feller et al.[12] and found to be relatively small in these situations (e.g., ∼0.5 kcal/mol for Li^+-OH_2 at the MP2(FC)/aug-cc-pVDZ computational levels) and, therefore, has been ignored in this work.[38]

The most demanding calculations were those for the transition metal monohydrates as a consequence of the various possible occupations of the d orbitals. It was not practicable to study all the possibilities for each monohydrate, although in most cases several electronic configurations were considered, see Table 1. For guidance as to the lower energy states of the monovalent monohydrates, $M[H_2O]^+$, extensive use was made of the work of Rosi and Bauschlicher.[8] These authors have pointed out that the overlap between the H_2O and the five components of the 3d orbitals on the metals is expected to be ordered according to $3d\delta(xy) \approx 3d\delta(x^2 - y^2) < 3d\pi(yz) < 3d\pi(xz) < 3d\sigma(z^2)$, where the symmetry axis is *z* and the molecule lies in the *yz* plane, see Figure 1. This ordering allows for the bending of the O−H bonds away from the metal ion, and as can be seen from Table 1, it is generally borne out at the MP2(FULL)/6-311++G** computational level.[8] A few calculations on the divalent monohydrates have been reported in the literature,[8,17,39,40] and these results have also been used for guidance wherever possible.

(36) Bader, R. F. W. *Atoms in Molecules, A Quantum Theory*; Oxford University Press: Oxford, 1990.

(37) (a) Cioslowski, J.; Nanayakkara, A.; Challacombe, H. *Chem. Phys. Lett.* **1993**, *203*, 137−142. (b) Cioslowski, J. *Chem. Phys. Lett.* **1994**, *219*, 151−154. (c) Cioslowski, J.; Mixon, S. T. *J. Am. Chem. Soc.* **1991**, *113*, 4142−4145.

(38) For comparison, at the MP2(FULL)/6-311++G**//MP2(FULL)/6-311++G** computational level, BSSE lowers the calculated binding enthalpy of $Al^{n+}-OH_2$ (n = 1, 2, 3) by 1.8, 1.9, and 0.5 kcal/mol, respectively.

(39) Bauschlicher, C. W.; Partridge, H. *J. Phys. Chem.* **1991**, *95*, 9694−9698.

Table 3. Bond Lengths (Å), Bond Angles (deg), and Bonding Enthalpies, ΔH°_{298} (kcal/mol) for the Metal Ion Monohydrates, $M^{n+}-OH_2$, Calculated at the MP2(FULL)/6-311++G**//MP2(FULL)/6-311++G** and {CCSD(T)(FULL)/6-311++G**//MP2(FULL)6-311++G**} Computational Levels[a]

			group										
			2A	3B	4B	5B	6B	7B	8	8	8	1B	2B
period	n		Ca^{n+}	Sc^{n+}	Ti^{n+}	V^{n+}	Cr^{n+}	Mn^{n+}	Fe^{n+}	Co^{n+}	Ni^{n+}	Cu^{n+}	Zn^{n+}
4	$n=1$	state	$^2A_1$	$^3A_1$	$^4B_2$	$^5A_1$	$^6A_1$	$^7A_1$	$^4B_2$	$^3B_1$	$^2A_1$	$^1A_1$	$^2A_1$
		M−O	2.390	2.193	2.114	2.069	2.115	2.206	2.019	1.973	1.952	1.945	2.063
		O−H	0.966	0.967	0.967	0.965	0.964	0.966	0.964	0.965	0.964	0.964	0.967
		∠HOH	103.9	106.0	106.5	106.9	105.7	107.5	106.1	106.6	107.2	107.1	107.1
		ΔH°_{298}	−27.6	−34.1	−34.7	−38.5	−30.5	−27.4	−35.9[b]	−37.2[d]	−41.1	−37.7	−31.8
			{−23.9}	{−34.4}	{−36.4}	{−41.8}	{−30.6}	{−27.7}	{−32.4}[c]	{−37.1}[e]	{−36.3}	{−36.1}	{−31.9}
	$n=2$	state	$^1A_1$	$^2A_1$	$^3B_2$	$^4A_2$	$^5A_1$	$^6A_1$	$^5A_1$	$^4B_2$	$^3A_1$	$^2A_1$	$^1A_1$
		M−O	2.277	2.124	2.056	2.026	1.958	2.006	1.940	1.899	1.880	1.832	1.874
		O−H	0.972	0.976	0.976	0.975	0.978	0.977	0.979	0.980	0.979	0.981	0.980
		∠HOH	101.2	104.2	104.8	105.4	106.3	105.5	106.3	106.9	107.7	108.8	108.2
		ΔH°_{298}	−51.9	−67.0	−70.5	−74.8	−84.3	−75.6	−85.5	−96.6	−92.9	−102.3	−94.7
			{−54.6}	{−66.5}	{−70.6}	{−74.7}	{−84.4}	{−75.7}	{−86.3}	{−94.7}	{−93.5}	{−102.5}	{−93.6}

[a] See footnotes to Table 1 for the geometrical parameters of isolated water. [b] At the MP2(FULL)/6-311++G** level, the lowest energy of Fe^+-OH_2 is for the $^4B_2$ state. [c] At the CCSD(T)(FULL)/6-311++G** level, the lowest energy of Fe^+-OH_2 is for the $^6A_1$ state. If the $^4B_2$ state is used ΔH°_{298} is −35.8 kcal/mol. The MP2(FULL)/6-311++G** geometrical parameters for the $^6A_1$ state are Fe^+-O, 2.117 Å; O−H, 0.967 Å; ∠HOH = 106.4°. [d] At the MP2(FULL)/6-311++G** level, the lowest energy of Co^+-OH_2 is for the $^3B_1$ state. [e] At the CCSD(T)(FULL/6-311++G** level, the lowest energy of Co^+-OH_2 is for the $^3A_2$ state. The MP2(FULL)/6-311++G** geometrical parameters for the $^3A_2$ state are Co^+-O, 2.003 Å; O−H, 0.964 Å; ∠HOH = 106.6°.

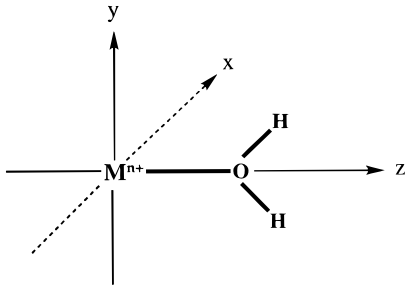

Figure 1. Coordinate system.

Results

A. Geometrical Parameters and Enthalpies of Hydration. With the single exception of the $^3A''$ excited state of Co^+-OH_2, see Table 1, the geometries of all the ground states and excited states of the main group and transition metal monohydrates we studied were found to be planar, see Figure 1.

The total molecular energies, thermal corrections, and entropies at the MP2(FULL)/6-311++G** computational level of all the monohydrates and metal ions we studied are given in Table 1S of the Supporting Information; total molecular energies at the CCSD(T)(FULL)/6-311++G**//MP2(FULL)/6-311++G** level are also given in Table 1S. An extensive comparison of our calculated geometrical parameters and bonding enthalpies of these metal ion monohydrates, with the calculated and experimental values of other authors, is given in Tables 2S and 3S of the Supporting Information. In those cases where a comparison can be made, there is generally good agreement between our calculated bonding enthalpies and experiment.

M−O and H−O bond distances, the HOH angles, and the bonding enthalpies for the main group metal ion monohydrates, $M^{n+}-OH_2$ with $n=1$ and 2, in groups 1A, 2A, 3A, and 4A of the first, second, and third periods are listed in Table 2, and the values for the transition metal ion monohydrates of the fourth period are given in Table 3. Data for Ca and Zn have been included in this table to provide baselines, Ca → Mn and Mn → Zn, from which the effect of adding the first five electrons and then an additional five electrons to the 3d orbital can be determined.

Chart 1

Sequence	M—O	O—H	∠HOH	ΔH°_{298}
Group 1A→ 2A→ 3A→ 4A	decr.	incr.	incr.	incr.
2nd Period → 3rd → 4th	incr.	decr.	decr.	decr.

Comparison of the geometrical parameters for unbound water and for the bonded H_2O in both the monovalent and divalent hydrates, see Tables 2 and 3, shows that the O−H bond length and the HOH angle are greater in all of the monohydrates except those of K^+-OH_2 and $Ca^{2+}-OH_2$. As the s and p valence shells are filled progressively in going from main group 1A → 2A → 3A → 4A, there is a general tendency for both of these water parameters to increase; whereas, in going from second period → third → fourth, there is a tendency for them to decrease. For the corresponding changes in group and period, the M−O bond length tends to decrease and increase respectively, and, as might be expected, the longer the M−O bond length the smaller the enthalpy of hydration. These relationships are summarized in Chart 1.

In Figure 2, ΔH°_{298} is plotted versus 1/M−O for the main group monovalent hydrates, M^+-OH_2, in the second, third and fourth periods, using total molecular energies from the CCSD(T)(FULL)/6-311++G**//MP2(FULL)/6-311++G** calculations and M−O distances and thermal corrections from the MP2(FULL)/6-311++G** optimizations and frequency analyses. When the points for the group 3A hydrates are omitted there is a linear dependency of the form

$$\Delta H^\circ_{298} = A + B(1/M-O) \qquad (1)$$

Values for the parameters A and B and the correlation coefficients r are listed in Table 4A. The anomalous behavior of the group 3A hydrates (see Figure 2) is connected with the presence of a formally fully occupied s shell in conjunction with a totally unoccupied p shell. The anomaly is such that for the

(40) Bauschlicher, C. W.; Sodupe, M.; Partridge, H. *J. Chem. Phys.* **1992**, *96*, 4453−4463.

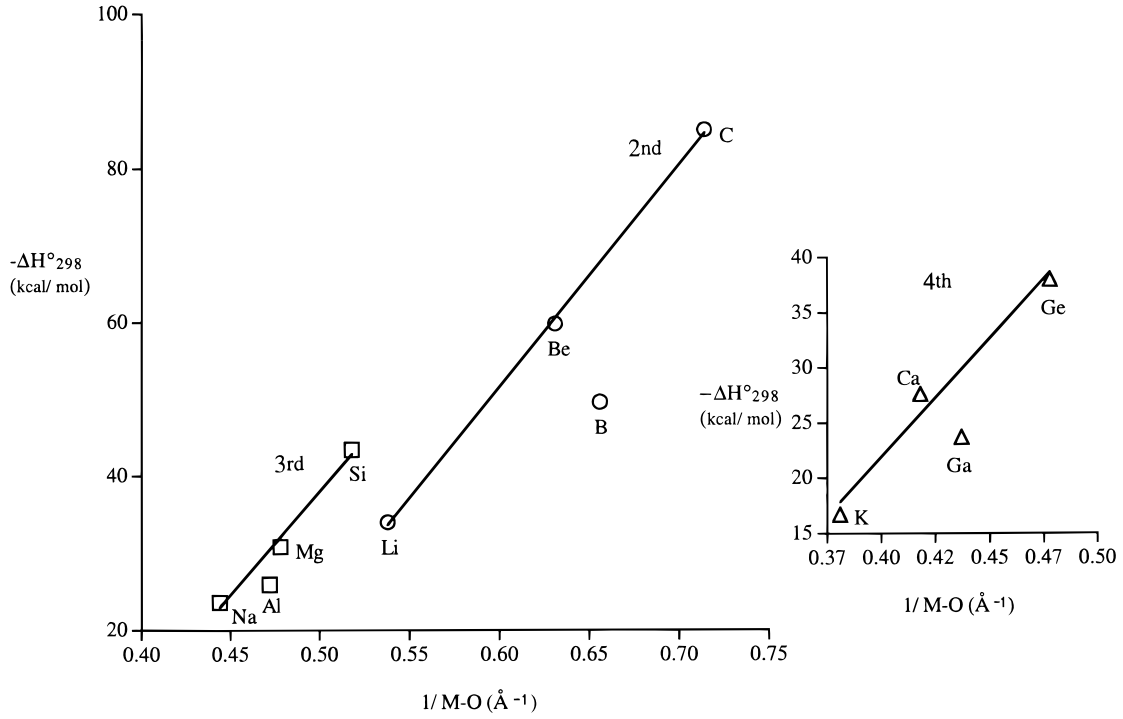

Figure 2. Plots of $-\Delta H^{\circ}_{298}$ versus 1/M−O for the main group metal ion monohydrates, $M^{+}-OH_2$ in groups 2A, 3A, and 4A in the second, the third, and the fourth periods, using energies from the CCSD(T)(FULL)/6-311++G**//MP2(FULL)/6-311++G** single-point calculations; thermal corrections and M−O distances were calculated at the MP2(FULL)/6-311++G**//MP2(FULL)/6-311++G** level. The anomalous behavior of the group 3A hydrates is connected with a formally fully occupied s shell in conjunction with a totally unoccupied p shell.

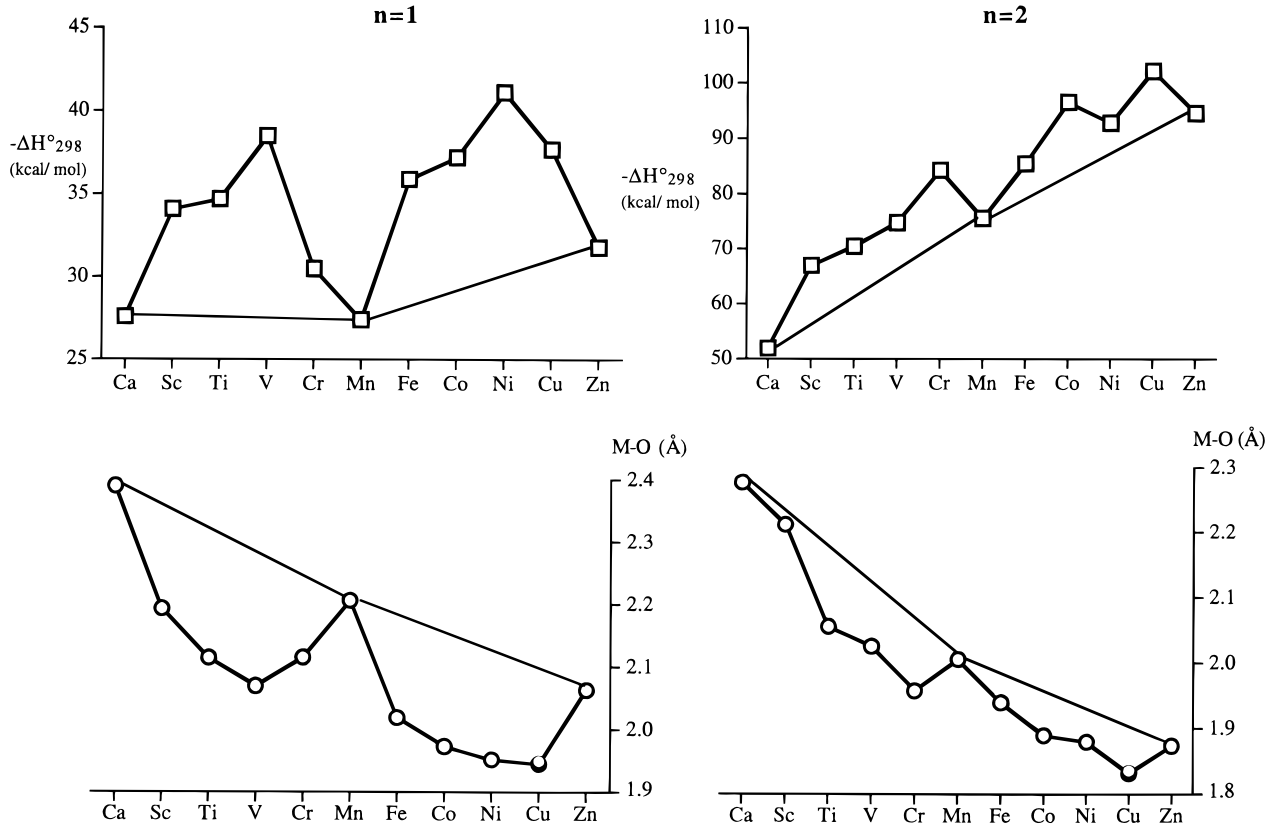

Figure 3. Variation of the enthalpy of hydration and the M−O bond distance for the monovalent ($n = 1$) and divalent ($n = 2$) transition metal ion monohydrates.

value of ΔH°_{298}, the M−O distance is smaller than expected, implying that for this particular electronic configuration the ion is more compact in relation to neighboring ions having valence shells with unpaired electrons.

The corresponding data for the divalent ions of the main group hydrates, $M^{2+}-OH_2$, show a similar anomaly. In this case it would appear that the M−O values for the group 4A ion—which likewise have a formally fully occupied s shell and a totally

Table 4. Parameters and Correlation Coefficients

(A) $\Delta H^\circ_{298} = A + B(1/\mathrm{M-O})$, Eq 1

metal ion sequence	MP2(FULL)/6-311++G**//MP2(FULL)/6-311++G** {CCSD(T)(FULL)/6-311++G**//MP2(FULL)/6-311++G**}		
	A	*B*	*r*[a]
$Li^+ \rightarrow C^+$	+122	−290	−1.00
	{+113}	{−274}	{1.00}
$Na^+ \rightarrow Si^+$	+96.5	−269	−0.99
	{+90.7}	{−256}	{−1.00}
$K^+ \rightarrow Ge^+$	−64.1	−215	−0.99
	{+61.8}	{−206}	{−1.00}
$Be^{2+} \rightarrow C^{2+}$	+545	−1032	−1[a]
	{+548}	{−1036}	{−1}
$Mg^{2+} \rightarrow Si^{2+}$	+228	−597	−1
	{+242}	{−625}	{−1
$Ca^{2+} \rightarrow Ge^{2+}$	+169	−502	−1
	{+152}	{−470}	{−1}
$Ca^+ \rightarrow Zn^+$	+26.5	−127	−0.82
	{+23.7}	{−119}	{−0.70}
$Ca^+ \rightarrow V^+$	+36.8	−154	−0.97
	{+84.2}	{−259}	{−0.99}
$Cr^+ \rightarrow Zn^+$	+65.3	−203	−0.96
	{+40.2}	{−149}	{−0.97}
$Ca^{2+} \rightarrow Zn^{2+}$	+158	−474	−0.99
	{+148	{−454}	{−0.99}

(B) $\Delta H^\circ_{298} = A' + B'\,\nu_{\mathrm{M-O}}$, Eq 3, and $\nu_{\mathrm{M-O}} = A'' + B''\,\Delta H^\circ_{298}$, Eq 4

metal ion	*n*	*A*′	*B*′	*A*″	*B*″	*r*[a]
transition	1	1.49	−0.100	26.5	−9.70	−0.98
	2	47.1	−0.256	189	−3.84	−0.99
second period	1	43.2	−0.138	333	−6.93	−0.98
	2	178	−0.313	574	−3.19	−1[b]
third period	1	22.1	−0.148	161	−6.43	−0.98
	2	52.1	−0.239	218	−4.19	−1[b]
fourth period	1	19.1	−0.166	115	−6.01	−1.00
	2	66.8	−0.311	215	−3.22	−1[b]

[a] Correlation coefficient. [b] Two-point data for groups 2A and 3A.

unoccupied p shell—are too small. Parameters for the linear equation based on the remaining points for the group 2A and 3A ions are also listed in Table 4A.

There is much less variation in the O−H bond length and HOH bond angle in the transition metal ion monohydrates as the 3d shell becomes filled in going from Sc^{n+} to Zn^{n+}, see Table 3, compared to values for main group metal ion hydrates. In the water moiety both bond lengths and angles are again greater in the hydrates than in unbound H_2O. For the monovalent and divalent ion hydrates the O−H bond lengths are fairly constant, 0.965 ± 0.001 and 0.978 ± 0.002 angstroms, respectively, and the HOH bond angle is also fairly constant for the monovalent ion hydrates, 106.7 ± 0.6°. However, for the divalent ion hydrates there is a slight tendency for the bond angle to be less for the lower atomic number ions, 105.2 ± 0.8° for Sc^{2+} to Mn^{2+} compared to 107.6 ± 1.0° for Fe^{2+} to Zn^{2+}. In marked contrast, the M−O bond distance and the enthalpy of hydration are affected to a far greater extent as the 3d shell becomes filled. In common with many other properties of transition metal compounds the ΔH°_{298} values follow a typical "double-humped" curve with respect to baseline values for Ca^{n+}, Mn^{n+}, and Zn^{n+} [41a−f] whereas the M−O bond distances lie on an inverted double-humped curve, see Figure 3. This double hump characteristic is due to the occupation of the 3d orbitals which project well out to the periphery of the metal ions and are thus able to influence their environment significantly; hence many of the properties of these ions with a partly filled d shell are quite sensitive to the number and arrangement of the d electrons present.[41g]

Even though the M−O distance and hydration enthalpy of the transition metal monohydrates vary with atomic number in such a complex manner, they are nevertheless inter-related via eq 1 as are the values for the main group metal ion hydrates. Plots of ΔH°_{298} versus 1/(M−O) are set out in Figure 4, using total molecular energies from the CCSD(T)(FULL)/6-311++G** calculations and M−O distances and thermal corrections from the MP2(FULL)/6-311++G** calculations. If all the monovalent hydrates, Ca^+-OH_2 through Zn^+-OH_2 are taken together the correlation coefficient is rather poor, −0.70, see Table 4A. But if they are taken in two groups, Ca^+-OH_2 through V^+-OH_2 and Cr^+-OH_2 through Zn^+-OH_2 far better linear plots are obtained, Figure 4a_1 and 4a_2, with correlation coefficients of −0.99 and −0.97, respectively. A distinguishing feature of the hydrates from Ca^+-OH_2 to V^+-OH_2 is that the lowest electronic states at both the MP2(FULL)/6-311++G** and CCSD(T)(FULL)/6-311++G** levels have one electron in the 4s orbital whereas, with the exception of Mn^+-OH_2, the lowest electronic states for Cr^+-OH_2 and Fe^+-OH_2 through Cu^+-OH_2 have the 4s orbital formally unoccupied. No such division for the divalent monohydrates is necessary since the 4s orbital

(41) (a) George, P.; McClure, D. S. *Prog. Inorg. Chem.* **1959**, *1*, 381−463. (b) *Ibid*., Table 10, p 416. (c) *Ibid*., Table 1, p 390. (d) *Ibid*., Table 2, p 391. (e) van Santen, J. H.; van Wieringen, J. S. *Rec. Trav. Chim.* **1952**, *71*, 420−430. (f) Phillips, C. S. G.; Williams, R. T. P. *Inorganic Chemistry*; Oxford University Press: New York, 1966; Vol. II, Chapter 24 and references therein. (g) Cotton, F. A.; Wilkinson, G. *Advanced Inorganic Chemistry*, 4th ed.; John Wiley and Sons: New York, 1980; Chapters 20 and 21.

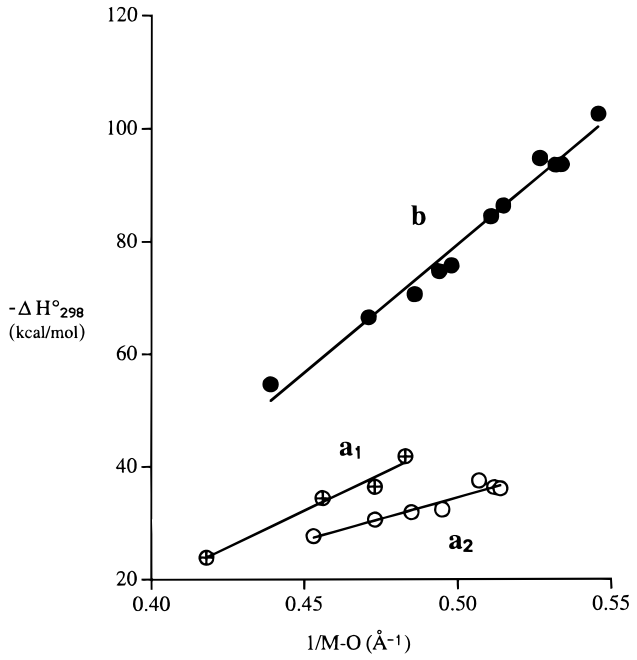

Figure 4. Plots of $-\Delta H^{\circ}_{298}$ versus 1/M−O for the monovalent transition metal ion monohydrates, (a_1) Ca^+ to V^+, (a_2) Cr^+ to Zn^+, and for the divalent ion monohydrates, (b) Ca^{2+} to Zn^{2+}.

is formally unoccupied in all these cases. The plot in Figure 4b with all the points taken together, Ca^{2+} through Zn^{2+}, has a correlation coefficient of −0.99.

It should be noted that Rosi and Bauschlicher[8] found that the lowest electronic state of Fe^+-OH_2 is a $^6A_1$ state with one electron in the 4s orbital. At the MP2(FULL)/6-311++G**// MP2(FULL)/6-311++G** level the lowest electronic state of Fe^+-OH_2 is a $^4B_2$ state and the $^6A_1$ state is nearly 10 kcal/mol higher in energy. At the CCSD(T)(FULL)/6-311++G**//MP2-(FULL)/6-311++G** level, however, the $^6A_1$ state is found to be lowest in energy, some 3.7 kcal/mol lower in energy than the $^4B_2$ state, see Table 1. There is also a discrepancy as to the lowest electronic state of Co^+-OH_2, but the energy differences at both computational levels are quite small, see Table 1.

B. Vibrational Frequencies. The vibrational modes for the monohydrates are depicted in Chart 2.[12] Vibrational frequencies for the main group metal ion monohydrates, M^+-OH_2 and $M^{2+}-OH_2$, calculated using the MP2(FULL)/6-311++G** computational level are listed in Supplementary Table 4S, and values for the transition metal ion monohydrates in Table 5S. For Li^+-OH_2, our calculated frequencies attributed to the water molecule within the complex of 1691, 3840, and 3924 cm^{-1} are in good agreement with those obtained experimentally; 1648, 3832, and 3943 cm^{-1}.[11]

The scissors mode, A_1, and the symmetrical and unsymmetrical H−O stretching modes, A_1 and B_2, are common to both bonded and free H_2O. Both of these stretching frequencies are smaller throughout groups 1A → 4A in the second, third and the fourth periods. Within these series, however, there is a difference. The A_1 and B_2 frequencies get progressively smaller in going from group 1A(2A) to group 4A; whereas both frequencies tend to increase in going from the second to the third, to the fourth period. The corresponding values for the transition metal ion mono- and divalent hydrates are also consistently smaller than those for free H_2O, but there seems to be no systematic variation with atomic number.

The wagging mode, B_1, the rocking mode, B_2 (and the M−O stretching mode, A_1) originate in the binding of the metal ion

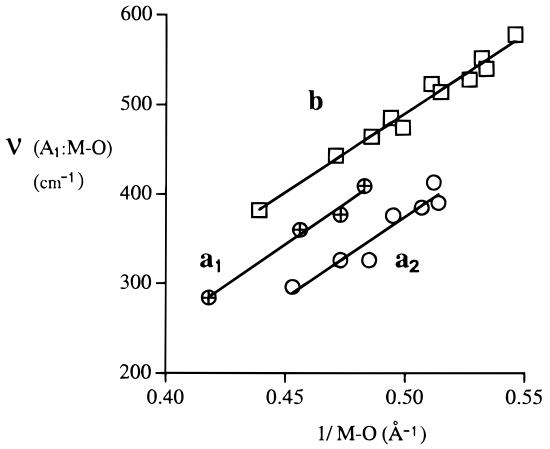

Figure 5. Plots of the M−O stretching frequency, A_1, versus 1/(M−O) for the monovalent transition metal ion monohydrates, (a_1) Ca^+ to V^+, (a_2), Cr^+ to Zn^+, and for the divalent metal ion monohydrates, (b) Ca^{2+} to Zn^{2+}.

Chart 2. Vibrational Modes[12]

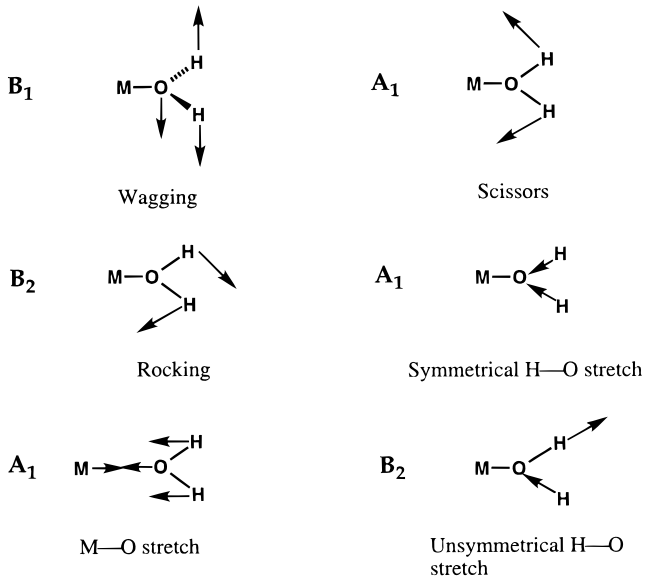

to the water. There are no apparent trends in the B_1 and B_2 frequencies for the main group monohydrates. With the transition metal monohydrates B_1 tends to decrease with increasing atomic number, but in an irregular manner. Nevertheless the values for the monovalent and the divalent ions of V and Cr, and likewise those for Ni and Cu, lie appreciably below the baselines defined by the values for Ca and Mn, and Mn and Zn, suggesting that there is an underlying *inverted* double-humped curve. The transition metal B_2 frequencies, on the other hand, follow the more common double-humped curve, see Figure 1S. Overall, these frequencies increase as the M−O distance decreases, like the bonding enthalpies shown in Figure 3 and are found to obey the corresponding inverse relationship,

$$\nu = A + B(1/M-O) \qquad (2)$$

(See Figure 2S and Table 6S of the deposited materials.)

The M−O stretching frequencies, A_1, for the mono- and the divalent transition metal ion monohydrates also follow double-humped curves, see Figures 3S and 4S, respectively. The values increase as the M−O distance decreases, and likewise obey an inverse relationship, see Figure 5 and Table 6S. In the case of the monovalent hydrates the values fall into two groups, Ca^+

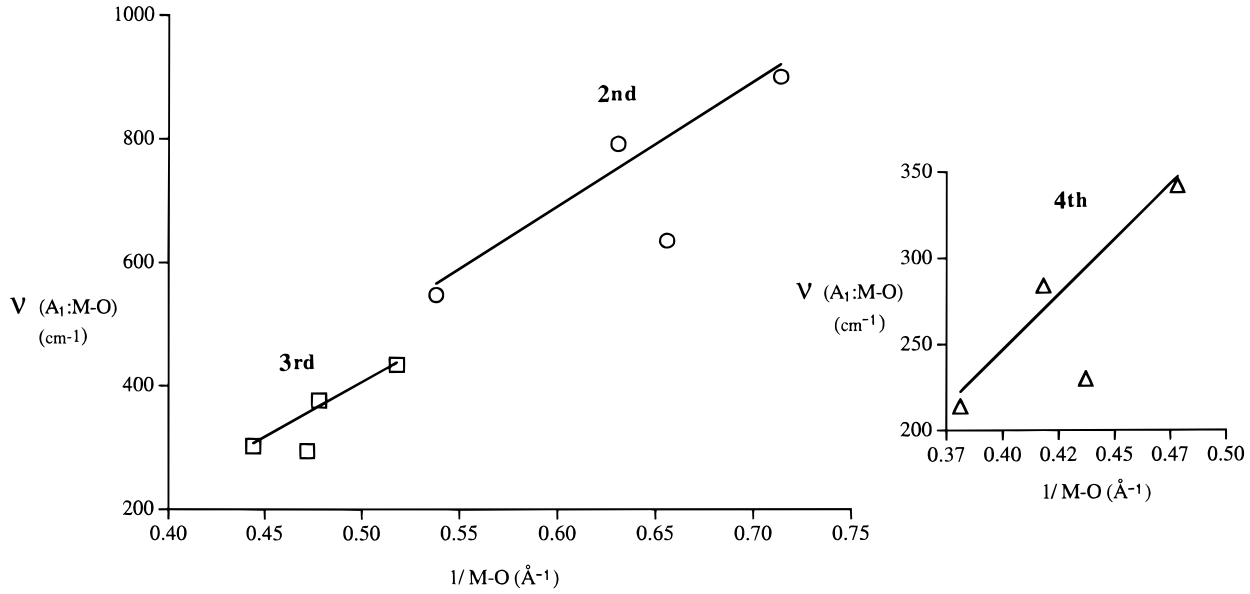

Figure 6. Plots of the M−O stretching frequency, A_1, versus 1/(M−O) for the monovalent main group metal ion monohydrates in group A of the second, third, and fourth periods.

to V^+, and Cr^+ to Zn^+, like the ΔH°_{298} values in Figure 4. Since ΔH°_{298} and the M−O stretching frequency both show an inverse dependence on the M−O distance, it follows that there should be a linear relationship between the two. Good linear plots are obtained in accord with the equations

$$H^\circ_{298} = A' + B'\nu_{M-O} \quad (3)$$

and

$$\nu_{M-O} = A'' + B''\,\Delta H^\circ_{298} \quad (4)$$

values for the parameters A′, B′, A″, B″ and the correlation coefficients are listed in Table 4B.

The M−O stretching frequencies for the main group metal ion monohydrates show similar behavior, although the values for the monovalent ions in group 3A and those for the divalent ions in group 4A, in which the outer valence shell is ns^2, appear to be abnormally low. See Figure 6 for the plots of ν_{M-O} versus 1/M−O for the monovalent ions, and Table 6S for the parameters and correlation coefficients in eq 2.

C. Orbital Occupancy. The metal orbital occupancy in the monohydrates of the main group and transition metal ions, calculated using natural population analysis (NPA) with the MP2(FULL)/6-311++G** densities are listed in Tables 7S and 8S respectively in the Supporting Information.

A common feature of the NPA analysis of the main group monohydrates is a small (typically less than 0.1) electron deficit in the valence orbital, *n*s, of the metal ion along with a definite electron presence in the (formally unoccupied) Rydberg orbitals. For example, in the case of Al^+-OH_2 we find $3s^{1.92}\ 3p^{0.10}\ 3d^{0.10}\ 4p^{0.01}$, for $Al^{2+}-OH_2$ we find $3s^{0.99}\ 3p^{0.12}\ 3d^{0.01}\ 4p^{0.01}$ and for $Si^{2+}-OH_2$ we find $3s^{1.91}\ 3p^{0.22}\ 3d^{0.02}\ 4s^{0.01}\ 4p^{0.01}$.

The valence orbital occupancy in the transition metal ion monohydrates—3d, together with 4s in the case of many of the monovalent hydrates—falls into three categories. In the first group, similar to the main group hydrates, the valence occupancy is *less* than the formal integral value. These include Cr^+-OH_2 to Zn^+-OH_2, and $Co^{2+}-OH_2$ to $Zn^{2+}-OH_2$. For example, we find Co^+-OH_2, $3d^{7.80}\ 4s^{0.11}\ 4p^{0.03}\ 4d^{0.10}\ 4f^{0.02}$. instead of the formally expected $3d^8\ 4s^0$ values. In the second group the occupancy is *greater* than the formal integral value, and this group includes Sc^+-OH_2, Ti^+-OH_2, V^+-OH_2 as well as $Sc^{2+}-OH_2$, $Ti^{2+}-OH_2$, and Cr^+-OH_2. Examples of this second group are Ti^+-OH_2 where the calculated orbital occupancy is $3d^{2.20}\ 4s^{0.87}\ 4p^{0.02}\ 4d^{0.02}\ 4f^{0.01}$ instead of the formal $3d^2\ 4s^1\ 4p^0$, and $Cr^{2+}-OH_2$ with an orbital occupancy of $3d^{4.08}\ 4s^{0.02}\ 4p^{0.02}\ 4d^{0.02}\ 4f^{0.01}$ instead of the formal $3d^4\ 4s^0$. In the third group, the values are the same, i.e., $Mn^{2+}-OH_2$, $3d^{5.0}$, and $Fe^{2+}-OH_2$, $3d^{6.0}$.

The occupancy in the oxygen and hydrogen orbitals in the hydrates provides an explanation for the trends in O−H bond lengths and HOH bond angles noted in section A, Table 2. The formation of the O−H bond is attributable to the overlap of the $2p_y$ and $2p_z$ atomic orbitals of the O-atom with the 1s orbital of the H atom, see Figure 1. Now the total occupancy in these orbitals (counting both H atoms) is found to *decrease* in going from Li^+ to C^+, i.e., 4.202, 4.168, 4.087, and 3.978, and from Na^+ to Si^+, i.e., 4.205, 4.185, 4.180, and 4.145, in accord with the observed *lengthening* of the O−H bond. The values for the divalent hydrates, Be^{2+} to C^{2+} and Mg^{2+} to Si^{2+}, show a similar decrease, namely 4.143, 3.976, 3.803 and 4.177, 4.120, and 4.098, respectively. On the other hand, the total occupancy in these orbitals is found to *increase* in going from the second to the third Period, in accord with the observed *shortening* of the O−H bond.

The monotonic *increase* in occupancy in the $2p_y$ orbital in conjunction with the *decrease* in occupancy in the $2p_z$ orbital accounts for the observed *increased* in the HOH bond angle in going from group 1A to 4A.

D. Atomic Charge Distribution. The NPA atomic charges from the MP2(FULL)/6-311++G** density on the metal, the oxygen, and the hydrogens—q_M, q_O, and q_H—in the mono- and divalent main group metal ions and the transition metal ions are listed in Tables 5 and 6; the values of q_O and q_H for unbound H_2O are −0.898 and +0.449, respectively. The corresponding AIM charges for a variety of main group monohydrates are given in Table 9S of the Supporting Information. These charges tend to show less charge transfer to the metal than those of the NPA charges.

Comparison of the values for the hydrate with those for unbound water shows that hydrate formation is consistently accompanied by an *increase* in the electronic charge on the

Table 5. Atomic Charges, q, on M, O, and H and the Transfer of Electronic Charge from the H_2O to the Metal Ion in the Main Group Metal Ion Monohydrates, $M^{n+}-OH_2$, with $n = 1$ and 2, Calculated from Natural Population Analyses (NPA) Using the MP2(FULL)/6-311++G** Densities

		$n = 1$				$n = 2$			
period	M	q_M	q_O	q_H	transfer	q_M	q_O	q_H	transfer
2	Li	+0.990	−1.019	+0.514	0.009	–	–	–	–
	Be	+0.964	−1.098	+0.567	0.036	+1.912	−1.153	+0.621	0.089
	B	+0.794	−0.978	+0.592	0.201	+1.609	−0.978	+0.684	0.390
	C	+0.559	−0.745	+0.593	0.441	+1.324	−0.785	+0.731	0.677
3	Na	+0.995	−0.992	+0.498	0.004	–	–	–	–
	Mg	+0.990	−1.040	+0.525	0.010	+1.968	−1.104	+0.568	0.032
	Al	+0.965	−1.027	+0.531	0.035	+1.876	−1.082	+0.603	0.124
	Si	+0.884	−0.987	+0.551	0.115	+1.845	−1.086	+0.620	0.154
4	K	+0.998	−0.974	+0.488	0.002	–	–	–	–
	Ca	+1.003	−1.028	+0.512	−0.004	+1.986	−1.075	+0.544	0.013
	Ga	+0.970	−1.003	+0.517	0.031	+1.840	−1.042	+0.601	0.160
	Ge	+0.902	−0.978	+0.538	0.098	+1.864	−1.063	+0.600	0.137

Table 6. Atomic Charges, q, on M, O, and H and the Transfer of Electronic Charge from the H_2O to the Metal Ion in the Transition Metal Ion Monohydrates, $M^{n+}-OH_2$, with $n = 1$ and 2, Calculated from Natural Population Analyses (NPA) Using the MP2(FULL)/6-311++G** Densities

	$n = 1$				$n = 2$			
M	q_M	q_O	q_H	transfer	q_M	q_O	q_H	transfer
Ca	+1.002	−1.034	+0.516	−0.002	+1.986	−1.075	+0.544	0.013
Sc	+0.953	−1.008	+0.527	0.046	+1.936	−1.060	+0.562	0.064
Ti	+0.945	−0.996	+0.525	0.054	+1.923	−1.049	+0.563	0.077
V	+0.928	−0.982	+0.526	0.070	+1.919	−1.050	+0.565	0.080
Cr	+0.971	−1.002	+0.516	0.030	+1.891	−1.039	+0.574	0.109
Mn	+0.980	−1.022	+0.521	0.020	+1.933	−1.074	+0.570	0.066
Fe	+0.971	−1.000	+0.519	0.038	+1.912	−1.071	+0.580	0.089
Co	+0.968	−1.015	+0.523	0.031	+1.902	−1.062	+0.580	0.098
Ni	+0.964	−1.014	+0.525	0.036	+1.901	−1.065	+0.582	0.099
Cu	+0.973	−1.026	+0.526	0.026	+1.875	−1.054	+0.590	0.126
Zn	+0.967	−1.025	+0.529	0.033	+1.919	−1.093	+0.587	0.081

oxygen and a (significantly larger) *decrease* in the electronic charge on the hydrogens. There is thus charge transfer from the water to the metal ion, see Tables 5 and 6. This transfer increases for both the mono- and divalent ions of the main group metal monohydrates in going from group 1 → 2 → 3→ 4, and decreases in going from second to the third and to the fourth period.

The charge on the metal, q_M, for both the mono- and divalent transition metal ion monohydrates follows an inverted double-humped dependency in going from Ca to Zn, see Figure 5S. This is reflected in the charge transfer which goes through two maxima in a corresponding double-humped curve, see Table 6.

Discussion

Two aspects of the present results call for further comment. First, the magnitude of the ligand field stabilization energies for the monohydrates of the divalent transition metal ions (calculated using the bonding enthalpies for $Ca^{2+}-OH_2$ and $Mn^{2+}-OH_2$, and $Mn^{2+}-OH_2$ and $Zn^{2+}-OH_2$ as baseline values) may be compared with the stabilization energies for multi-ligand species such as the aquo-ions $[M^{2+}(H_2O)_6]$aq and halide and oxide crystal lattices. Taking the values for Fe^{2+}, Co^{2+}, Ni^{2+}, and Cu^{2+}, for example, we have calculated the ligand field stabilization energies for these monohydrates to be 6, 13, 6, and 11 kcal/mol, respectively (from Figure 4) compared to the experimental values for the aquo-ions 17, 24, 34, and 25 kcal/mol;[41b] for the fluoride crystal lattice 26, 28, 38, and 29 kcal/mol;[41b] for the chloride crystal lattice 16, 25, 30, and 28 kcal/mol;[41c] and for the oxide crystal lattice 18, 23, 36, and 32 kcal/mol.[41d] The bonding of just one water molecule thus accounts for a substantial fraction of the stabilization energy of the hexacoordinated aquo-ion, and it is perhaps surprising that the values are as large as they are in relation to those for the charged species F^-, Cl^-, and O^{2-}.

Second, the bonding enthalpies and the vibrational frequencies for the M−O bond in the monohydrates are very similar to the bond energies (Laidler parameters) and vibrational frequencies for covalent bonds such as C−S, C−Cl, and C−Br, i.e., 70 kcal/mol and 600−700 cm^{-1}, 84 kcal/mol and 600−800 cm^{-1}, and 71 kcal/mol and 500−600 cm^{-1}, respectively.[42,43]

Concluding Remarks

Our main findings are described in the following points.

(i) With the single exception of the 3A″ excited state of Co^+-OH_2, all the hydrates studied are planar at the MP2(FULL)/6-311++G** level.

(42) Cox, J. D.; Pilcher, G. *Thermochemistry of Organic and Organometallic Compounds*; Academic Press: London, 1970; p 592.
(43) Bellamy, L. J. *The Infrared Spectra of Complex Molecules*, 2nd ed.; Methuen & Co. Ltd.: London, 1966; pp 329 and 354.
(44) Davy, R. D.; Hall, M. B. *Inorg. Chem.* **1988**, *27*, 1417−1421.
(45) Wojcik, M. J.; Mains, G. J.; Devlin, J. P. *Int. J. Quantum Chem.* **1995**, *53*, 49−56.
(46) Kim, J.; Lee, S.; Cho, S. J.; Mhin, B. J.; Kim, K. J. *J. Chem. Phys.* **1995**, *102*, 839−849.
(47) Bauschlicher, C. W., Jr.; Partridge, H. *J. Phys. Chem.* **1991**, *95*, 9694−9698.
(48) Bauschlicher, C. W., Jr.; Sodupe, M.; Partridge, H. *J. Chem. Phys.* **1992**, *96*, 4453−4463.
(49) Cachau, R. E.; Villar, H. O.; Castro, E. A. *Theor. Chim. Acta* **1989**, *75*, 299−306.
(50) Searlin, S. K.; Kebarle, P. *Can. J. Chem.* **1969**, *47*, 2619−2627.
(51) Kochanski, E.; Constantin, E. *J. Chem. Phys.* **1987**, *87*, 1661−1665.
(52) $Fe[OH_2]^+$ in the $^6A_1$ state.
(53) Schultz, R. H.; Crellin, K. C.; Armentrout, P. B. *J. Am. Chem. Soc.* **1991**, *113*, 8590−8601.

(ii) In general, the trends in the various properties can be correlated with the progressive occupancy of the s, p, and d orbitals.

(iii) In particular, attributing the formation of the O−H bond to the overlap of the $2p_y$ and $2p_z$ atomic orbitals of the O atom with the 1*s* orbital of the H-atom, the trends in O−H bond length and ∠HOH for the main group hydrates can be accounted for by the progressive changes in the total electron occupancy in these orbitals.

(iv) In going from Ca to Mn to Zn the properties of the transition metal ion monohydrates follow typical "double-humped" curves.

(v) Both the enthalpies of formation and the M−O stretching frequencies are inversely proportional to the M−O distance: thus the stronger the bonding in the hydrate the larger the stretching frequency for the M−O bond.

(vi) Comparison of the distribution of atomic charge on the unbound water molecule with the distribution in the hydrates shows that hydrate formation is consistently accompanied by a small but definite increase in the electronic charge on the oxygen and a (significantly larger) decrease in electronic charge on the hydrogens, so that there is a net transfer of charge from the water to the metal ion.

(vii) With the exception of Fe^+-OH_2 and Co^+-OH_2, the MP2(FULL)/6-311++G**//MP2(FULL)/6-311++G** and CCSD(T)(FULL)/6-311++G**//MP2(FULL)/6-311++G** calculations find the same electronic configurations for the ground states of the first-row mono- and divalent transition metal monohydrates. Furthermore, the calculated binding enthalpies of *corresponding* states of these monohydrates are generally in good agreement at both computational levels, with the largest difference, 4.8 kcal/mol, involving Ni^+-OH_2 where the d shell is nearly complete.

Acknowledgment. We thank the Advanced Scientific Computing Laboratory, NCI-FCRF, for providing time on the CRAY YMP supercomputer. This work was supported by Grants CA10925 (to J.P.G.), GM31186 (to G.D.M.), and CA06927 (to F.C.C.C.) from the National Institutes of Health and by an appropriation from the Commonwealth of Pennsylvania (to F.C.C.C.). The authors gratefully acknowledge the technical assistance of Carol Afshar. The contents of this paper are solely the responsibility of the authors and do not necessarily represent the official views of the National Cancer Institute.

Supporting Information Available: Tables listing the molecular energies, entropies and thermal corrections for the metals and monohydrates; comparisons between calculated and observed geometrical parameters, enthalpies and binding energies; vibrational frequencies in cm^{-1} for the main and first transition group metal ion monohydrates; parameters *A* and *B* and correlation coefficients, *r*, for linear plots relating ν to 1/(M−O); orbital occupancy for main group and first-row transition metal monohydrates; charges derived from Bader's AIM approach, and figures showing the variation of the H_2O rocking frequency, B_2, for the mono- and divalent transition metal ion monohydrates from Ca to Zn; plots of the H_2O rocking frequency, B_2, versus 1/M−O for the mono- and divalent transition metal ion monohydrates; the variation of the M−O stretching frequency, A_1, and the M−O distance for the mono- and divalent transition metal monohydrates; and the variation of the atomic charge on the metal for the mono- and divalent transition metal monohydrates are available (30 pp). Ordering information is given on any current masthead page.

IC971613O